One and two dimensional self-assembly of comb-like amphiphilic copolyelectrolytes in aqueous solution

C. Limouzin-Morel, F. Dutertre, W. Moussa, C. Gaillard, I. Iliopoulos, D. Bendejacq*, T. Nicolai and C. Chassenieux

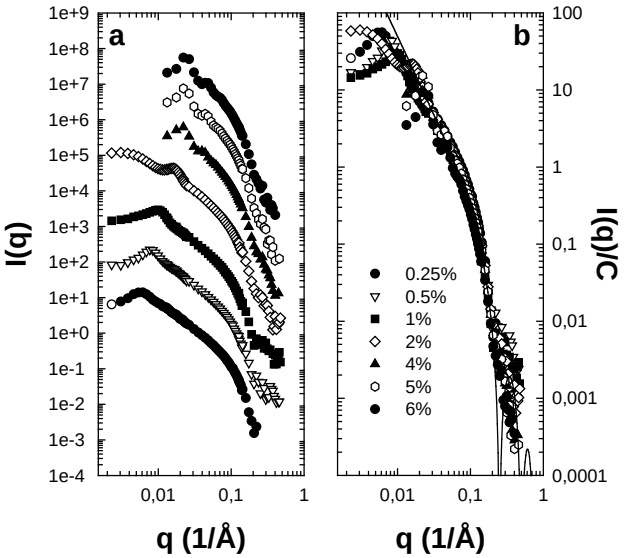

Figure S1: Scattering data obtained from SANS for 45C16 at different concentration in D_20. In figure a) the curves have been shifted vertically for clarity , while in figure b) the data have been normalized by concentration. The solid line in figure b corresponds to a fit of the data with the form factor of lamellae (eq.1).

Figure S2 : Freeze-fracture TEM image of a suspension of 45C16 at C=10 wt% in a (2/3-1/3) H_2O-glycerol mixture. The scale bar represent 200nm

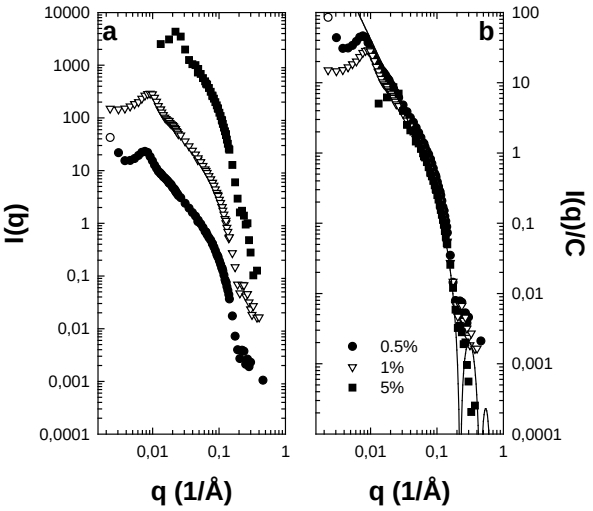

Figure S3: Scattering data obtained from SANS for 45C18 at different concentration in D20 a) The curves have been shifted vertically for clarity , while in figure b) the data have been normalized by concentration. The solid line in figure b corresponds to a fit of the data with the form factor of lamellae (eq.1).

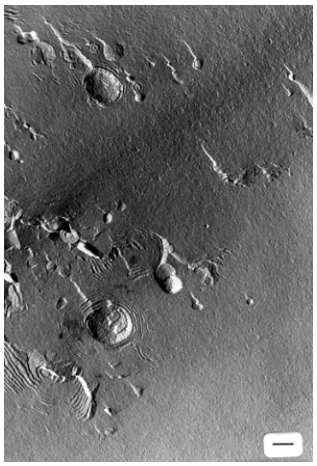

Figure S4 : Freeze-fracture TEM image of a suspension of 45C18 at C=7 wt% in a (2/3-1/3) H2O-glycerol mixture. The scale bar represent 230nm

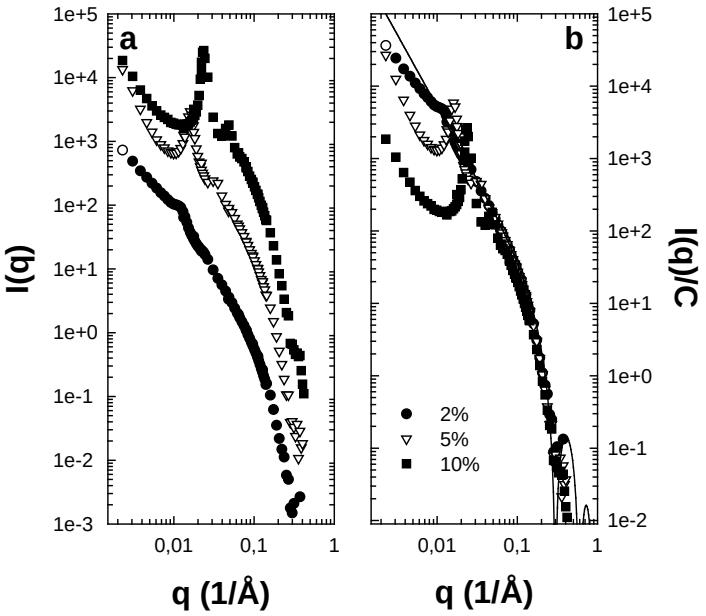

Figure S5: Scattering data obtained from SANS for 35C12 at different concentration in D20 a) The curves have been shifted vertically for clarity , while in figure b) the data have been normalized by concentration. The solid line in figure b corresponds to a fit of the data with the form factor of lamellae (eq.1)

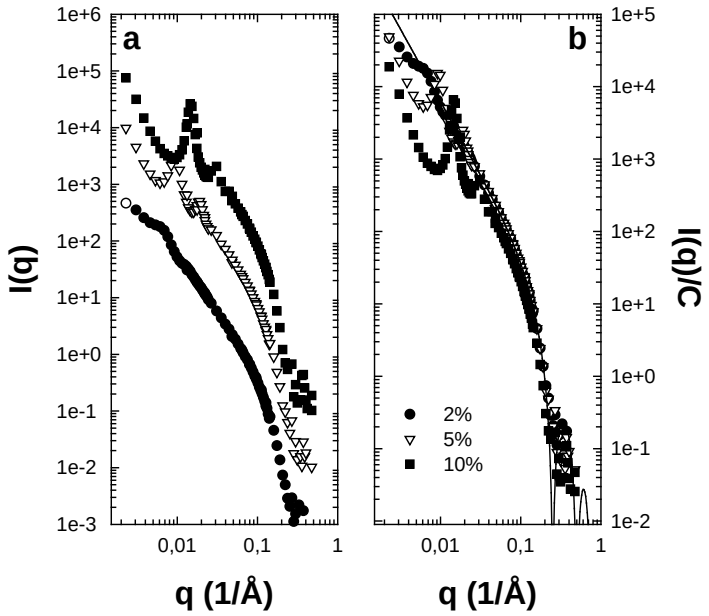

Figure S6: Scattering data obtained from SANS for 35C16 at different concentration in D20 a) The curves have been shifted vertically for clarity , while in figure b) the data have been normalized by concentration. The solid line in figure b corresponds to a fit of the data with the form factor of lamellae (eq.1).

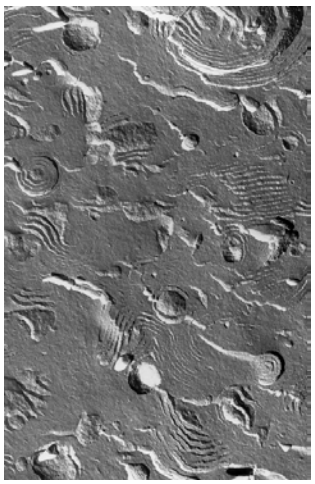

Figure S7: freeze-fracture TEM on a 35C16 at 7wt% in a {2/3-1/3} H2O-glycerol mixture. The scale bar represents 200nm

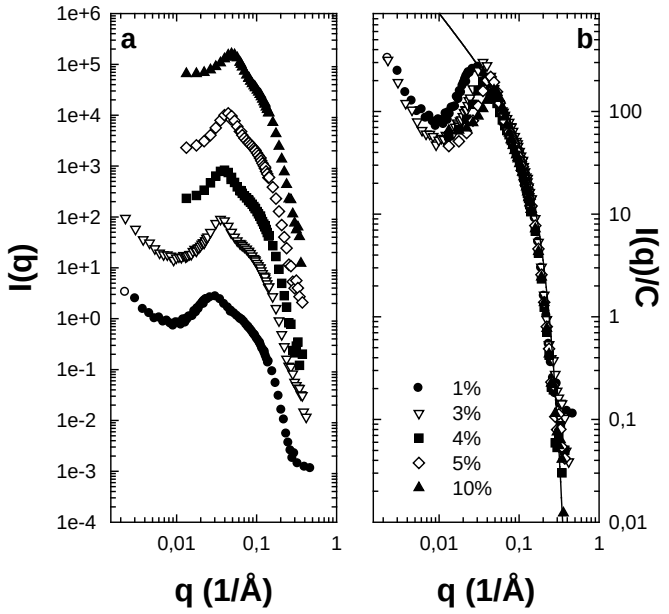

Figure S8: Scattering data obtained from SANS for 65C12 at different concentration in D_20. In figure a) the curves have been shifted vertically for clarity , while in figure b) the data have been normalized by concentration. The solid line in figure b corresponds to a fit of the data with the form factor of cylinders (eq.3)

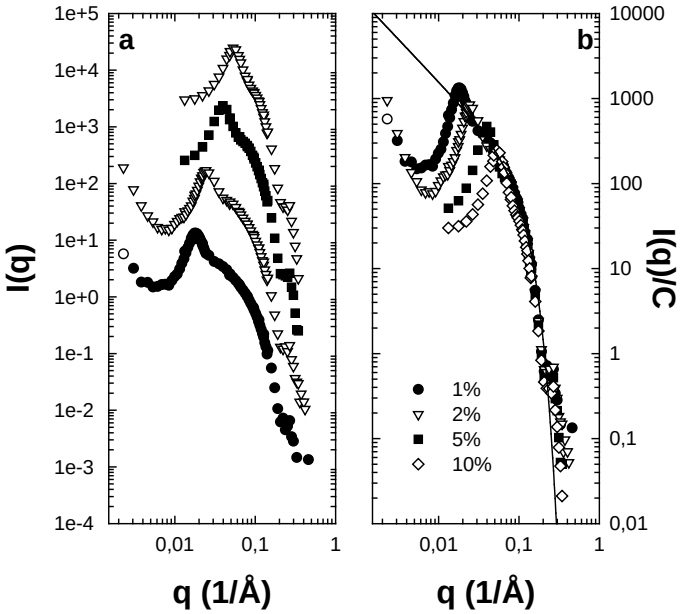

Figure S9: Scattering data obtained from SANS for 65C16 at different concentration in D_20. In figure a) the curves have been shifted vertically for clarity , while in figure b) the data have been normalized by concentration. The solid line in figure b corresponds to a fit of the data with the form factor of cylinders (eq.3)

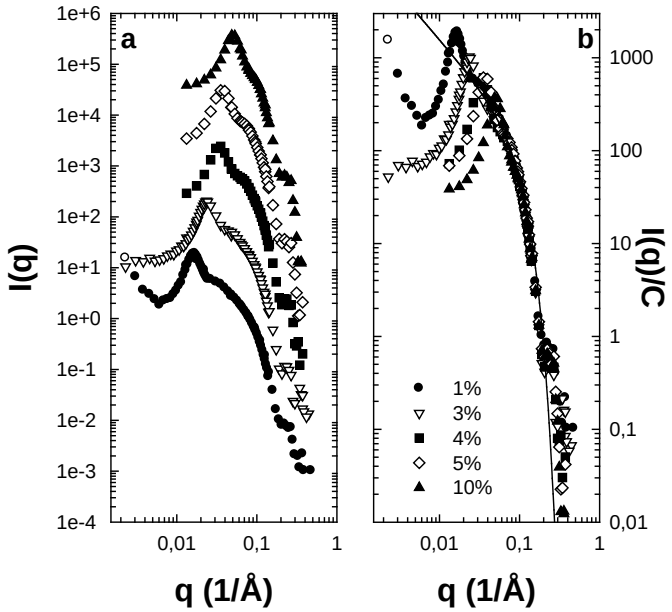

Figure S10: Scattering data obtained from SANS for 65C18 at different concentration in D_20. In figure a) the curves have been shifted vertically for clarity , while in figure b) the data have been normalized by concentration. The solid line in figure b corresponds to a fit of the data with the form factor of cylinders (eq.3)

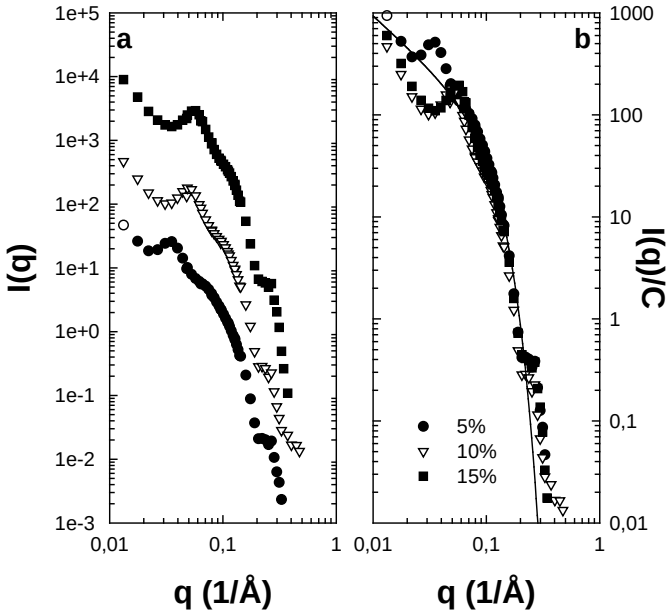

Figure S11: Scattering data obtained from SANS for 80C16 at different concentration in D_20. In figure a) the curves have been shifted vertically for clarity , while in figure b) the data have been normalized by concentration. The solid line in figure b corresponds to a fit of the data with the form factor of cylinders (eq.3).

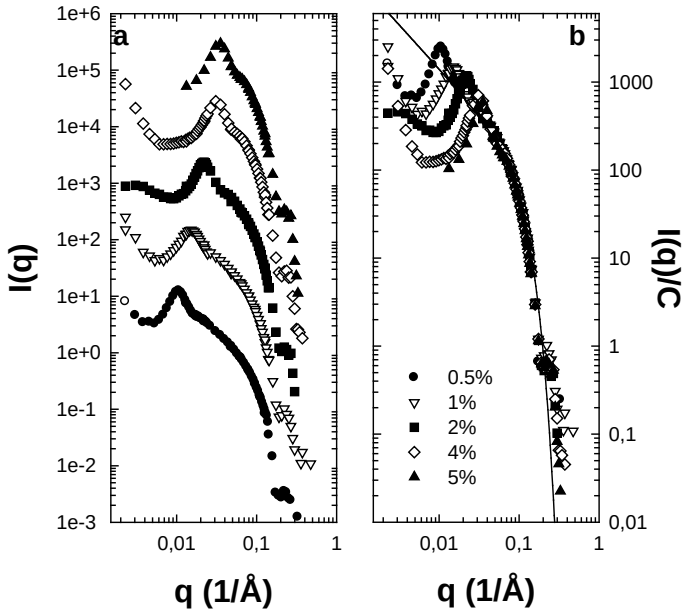

Figure S12: Scattering data obtained from SANS for 80C18 at different concentration in D_20. In figure a) the curves have been shifted vertically for clarity , while in figure b) the data have been normalized by concentration. The solid line in figure b corresponds to a fit of the data with the form factor of cylinders (eq.3).